Journal of Applied Fluid Mechanics, Vol. 17, No. 12, pp. 2761-2774, 2024.
Available online at www.jafmonline.net, ISSN 1735-3572, EISSN 1735-3645.
https://doi.org/10.47176/jafm.17.12.2678

Response Analysis of River Ice-induced Vibration under Fluid-solid Coupling

Z. Zhang [1,2†], J. Song[1] and K. Wang [1]

[1] *School of Water Conservancy and Civil Engineering, Northeast Agricultural University, Harbin 150000; China*
[2] *School of Civil Engineering, Harbin Institute of Technology, Harbin 150000, China*

†Corresponding Author Email: zhangzhonghao@neau.edu.cn

ABSTRACT

Significant progress has been made in understanding the mechanisms and simulations of ice-induced shock vibrations due to continuous experimentation and simulation of vibrations induced by ocean platforms. However, the threat of such vibrations to bridges in cold regions with spring rivers remains significant. Currently, challenges persist in the numerical analysis methods applied to vibrations caused by collisions between ice and bridges in river channels. This difficulty primarily arises from the insufficient consideration of the impact of flow field coupling on ice-induced shock vibrations under various simulation conditions. This paper aims to analyze the influence of ice-induced shock vibrations arising from collisions involving bridges, ice, water, and air. It also compares the Semi-Arbitrary Lagrangian-Eulerian (S-ALE) and Arbitrary Lagrangian-Eulerian (ALE) methods, finding that the S-ALE method is better suited for complex flow-solid coupling analysis under the same model. Comparative analysis shows that the fluid effect period increased by approximately 30%, resulting in an 8% reduction in peak values. This confirms the applicability of the ice-induced shock vibration theory and demonstrates that factors such as velocity and thickness significantly impact these vibrations. The findings offer valuable insights for the numerical simulation of river ice-induced shock vibrations due to bridge-ice collisions in cold areas.

Article History

Received March 4, 2024
Revised June 1, 2024
Accepted July 4, 2024
Available online October 2, 2024

Keywords:

Dynamic response
Fluid-solid coupling
Ice shock vibration
Numerical simulation
S-ALE method

1. INTRODUCTION

Rivers in cold regions undergo a thawing period each spring following the winter freeze. During this period, drifting ice bodies form and flow downstream, impacting hydraulic structures in the river. These ice collisions can cause wear and tear on structures, reduce their service life, and may even lead to dislocations between supports and beam bodies, deformation and fracture of expansion joints, and in extreme cases, compromise the stability and integrity of rivers and bridges, potentially leading to the collapse of hydraulic structures and severe casualties. Therefore, this paper focuses on the numerical simulation and analysis of the ice-induced vibration response of bridge piers in cold regions.

Since the 1960s, three basic response modes of ice shock vibration have been identified: indirect breaking, frequency locking, and continuous breaking (Xu & Erkan 2018). These studies highlight how the characteristics of ice floe destruction and structural vibration vary with the velocity of the ice flow. Marine platform vibration was first studied in the Bohai Sea during oil exploration and exploitation activities in China (Yue, et al. 2008), marking the beginning of research into ice shock vibration.

In 1986, Sodhi & Morris (1986) conducted a small-scale experiment and observed that as flowing ice moves through a rigid cylindrical structure at varying speeds, the linear relationship between the characteristic frequency of the continuous ice-breaking force and the ice velocity-to-ice thickness ratio is minimally affected by the cylinder's diameter. They concluded that the average length of the damaged area is approximately one-third of the ice thickness. In 1988, Jordaan (1988) performed a medium-sized test where he found that when drift ice rapidly compresses against a structure at a constant speed, the periodic variations in the moving ice load correlate with the ice sheet breaking. Jordan highlighted that the primary mechanisms of energy dissipation during the load cycle include the viscous extrusion of crushed ice grains, the elastic stored energy in both ice and structures, and minor surface energy from ice fragmentation. In 1989, Karna & Turunen (1989) investigated an offshore structure's ice

shock vibration model, which characterized the nonlinear coupling between fragmentation and clearing processes. In 1994, Kennedy et al. (1994) noted that in a series of medium-sized tests, the extrusion of broken ice coincided with the peak breaking load of the ice sheet, whereas slow extrusion correlated with the non-peak stages. In 2001, Devinder (2001) conducted small-sized tests to measure the pressure between freshwater ice rows and structures, gathering data on the interaction and response of ice forces at different ice speeds. This paper provided insights into how ice force varies with ice speed. In 2015, Kashfi et al. (2015) conducted destruction tests on freshwater ice cone samples, gaining a deeper understanding of the load and dynamic characteristics of ice during compressive destruction. The tests also revealed peeling and crushing behaviors of ice and various degrees of recrystallization within the compression areas. In 1995, Cai Zhirui et al. (1995) focused on the dynamic response of drift ice impacting the Jiamusi Songhua River Highway Bridge, determining the drift ice load through dynamic displacement. In 2002, Ou et al. (2002) of Harbin Institute of Technology proposed a unified static ice force model that simplifies the treatment of different types of ice row destruction, including extrusion, buckling, and bending. The model also analyzed conditions conducive to self-excited vibration. Yue et al. (1999) from Dalian University of Technology demonstrated in 1999 that in ice-induced vibrations of cone structures, the ice sheet primarily fails due to bending, exhibiting noticeable periodicity and dynamic amplification. In 2000 and 2005, Yue & Bi (2000) analyzed the vibration of ice-breaking cone and cylindrical structures and (Yue et al. 2005) observed the toughness and brittle transition of sea ice under uniaxial loading. In the ductile zone, the compressive strength of ice increases as the strain rate decreases, stabilizing in the brittle zone. This transition is crucial for further studies. In 2006, Qu (2006) investigated random ice loads on marine structures through field data analysis. In 2012, Dong (2012) conducted model tests to explore the effects of ice forces on upright round piles and pile structures and to simulate protection facilities for typical and sloped structures. In 2017, Wang (2017) obtained data on the bending strength and elastic modulus of natural ice through in-situ cantilever tests, further refining the comprehensive coefficient in the ice force calculation formula through model testing. These studies are pivotal for understanding and predicting the random ice loads on marine structures, the characteristics of ice forces on impact structures, and the interactions between natural ice and vertical structures. They provide a vital foundation for engineering design in related fields. In 2019, Kehua et al. (2019) investigated the coupling effect of aerodynamic loads and ice-induced vibrations on offshore wind turbine generators. The frequency domain response results indicated that ice-induced vibrations significantly affect the vibration of wind turbine towers. In 2021, Zhu et al. (2021) explored the combined effects of dynamic ice loads, tidal current resistance, and wind load on offshore wind turbines. Their study, which utilized self-excited vibration theory, concluded that the frequency of sea ice was "locked" onto the first frequency of the wind turbine.

In recent years, scholars have increasingly deepened their study of the interactions between ice and structures. Significant advances have been made in theoretical modeling, numerical simulation, and experimental research, enhancing both academic research and practical applications in ice shock vibration. However, challenges remain in the field. Firstly, most research focuses on sea ice, whose mechanical properties differ from those of river ice. Consequently, findings related to the ice-induced vibrations of offshore platforms cannot be directly applied to rivers. Additionally, studies on ice-induced vibrations in cold regions often lack empirical data, leading researchers to rely on numerical simulations and theoretical studies that seldom account for the influence of fluid dynamics.

This paper innovatively incorporates mechanical characteristics such as the ductile-brittle transition of river ice and employs the advanced S-ALE. This method effectively couples fluid dynamics with impact dynamics, advancing research on ice-induced vibrations of river ice and bridge piers. By analyzing the dynamic curve outputs of piers, we gain a deeper understanding of the mechanisms and characteristics of ice-induced vibration with fluid interaction in rivers. Furthermore, this paper compares the S-ALE method with the traditional ALE method, demonstrating the superior performance of S-ALE in handling such issues and briefly exploring how the properties of the ice affect ice-induced vibrations. This paper provides a theoretical reference for understanding the vibration characteristics of hydraulic structures exposed to ice.

2. THE DYNAMIC RESPONSE MODEL

This paper employs numerical simulation to study ice-induced vibration. This method effectively addresses natural phenomena that occur under specific conditions and are difficult to measure directly. LS-DYNA, an advanced explicit nonlinear dynamic analysis software, is extensively used to simulate various complex nonlinear problems in the real world. Particularly useful for impact dynamics problems, the software can also handle fluid-solid coupling using ALE and S-ALE methods. The choice of S-ALE in this research is motivated by its convenience and accuracy. Yu et al. (2011) conducted a detailed field test on the ice impact force on Pier No. 10 of the Jiamusi Bridge over the Songhua River on April 12, 2009, providing valuable experimental data for theoretical analysis. In this paper, the measured data are used for simulation, and the reliability of the numerical simulation is validated by comparing the peak ice force, facilitating a thorough discussion on the vibration response during the collision process.

2.1 Ice Body Model

The destruction characteristics of river ice exhibit distinct patterns, varying with temperature and strain rates during testing. In engineering terms, materials that undergo less than 5% plastic deformation before fracturing are generally classified as brittle. Under low strain rates, ice failure tends to exhibit toughness, often resulting in swelling failure after compression.

Table 1 Ice body model, calculated parameters

	Ice
Density/（kg/m^3）	910
Young modulus/（GPa）	2.2
Plastic hardening modulus/（GPa）	4.26
yield stress/（MPa）	2.12
Poisson ratio	0.31
failure criterion	0.35

Conversely, at high strain rates, the ice becomes brittle, and the failure mode demonstrates increased brittleness. Ice may experience only brittle failure at very low strain rates, while it displays brittle transition characteristics at intermediate rates.

The isotropic elastic fracture failure model is used in LS-DYNA simulations to describe the constitutive relationship with strain rate during impact. Specifically, the plastic strain failure criterion * MAT_STRAIN_RATE_DEPENDENT_PLASTICITY is adopted. This model simulates the behavior of materials under different strain rates effectively. In this paper, the *MAT_ADD_EROSION option is used to simulate ice breaking, controlling the principal tensile stress at 0.8 MPa. Elements exceeding this stress threshold are deleted to prevent the subsequent effects of interference and to reduce both the computational load and the possibility of errors. This method not only minimizes the occurrence of adverse volume issues but also simplifies computational complexity. Many constitutive models in LS-DYNA do not inherently include failure, which makes the *MAT_ADD_EROSION option valuable for introducing failures into these models. The scheme is highly versatile and suitable for various constitutive models with differing failure and erosion criteria.

According to the competitive model of dislocation slip and cleavage fracture proposed by Rice and Thomson (1974), when the strain rate is very low, the main cause of material damage is internal dislocation slip. At this rate, the ice undergoes plastic deformation and does not exhibit rapid crack propagation, which contributes to the toughness of the ice. Under conditions of high strain rate, internal dislocation slip does not have enough time to complete within the sample. Consequently, the ice primarily undergoes cleavage, and the cracks expand rapidly, rendering the material brittle. However, there are few studies on the mechanical properties of river ice, with the majority focusing on sea ice. Many factors influence the mechanical properties of ice and demonstrate significant specificity, making it challenging to apply findings from sea ice studies to address common problems of river ice-structure interaction in China. Therefore, to study the interaction between local fluid and bridge pier structures in cold areas, it is necessary to use the unique ice bodies found in these regions for experimentation. This paper focuses on Songhua River ice, drawing inspiration from the research findings of Yin (2019) and Oxford (2018). The ice body parameters obtained indicate that the compressive strength generally reaches its peak at about 1 × 10 $^{-3}$ MPa when the loading rate is lower than this value. When the loading rate is less than 1 × 10 $^{-3}$ MPa, strength

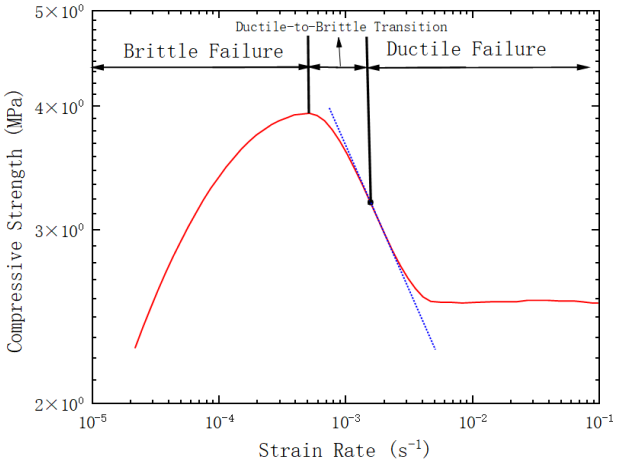

Fig. 1 Compressive strength and strain rate fitting curve

is positively correlated with the loading rate, and when the loading rate exceeds 1 × 10 $^{-3}$ MPa, the strength is negatively correlated with the loading rate. The ultimate compressive strength of ice increases gradually in the temperature range from 0 ℃ to -20 ℃, especially between -3 ℃ and -5 ℃, highlighting the sensitivity of ice strength to temperature changes. This paper, targeting the melting period in early spring, considers the brittleness transition curve of the ice layer at 0 ℃.

For computational convenience, this paper employs Python programming to fit the intensity and strain rate curve obtained from uniaxial compression experiments on river ice, as reported by Oxford (2018). The resulting curve, shown in Fig. 1, facilitates the easy retrieval of compressive strength corresponding to different rates for subsequent substitution in calculations.

In the interaction with the actual structure, ice forces rarely reach the maximum at a specific strain rate. Therefore, it is necessary to describe the material properties of river ice more accurately. However, for the purposes of this paper, we must assume a fixed compressive strength at a specific strain rate, which simplifies the complexity of the research.

The accuracy of the calculation results depends on the grid size, but using an excessively small grid size will undoubtedly increase the computational workload. Considering that the peak ice force from impact failure is much larger than that from extrusion, the critical part of the collision simulation is located at the interface between the ice sheet and the bridge pier. Thus, the ice strip grid in this area needs to be appropriately refined. Initially, the entire ice body must be meshed.

Yu et al. (2011) suggests that enhancing calculation efficiency and accuracy requires determining reasonable lengths for the ice sheet in the flow direction and perpendicular to the flow. The analysis indicates that the lengths of the ice sheet in the flow direction and perpendicular to the flow should be at least 25% and 10%, respectively, of the corresponding ice sheet dimensions (2.6 times the half-width of the pier). Based on this, the total dimensions of the ice body are 8 m × 6 m × 0.5 m.

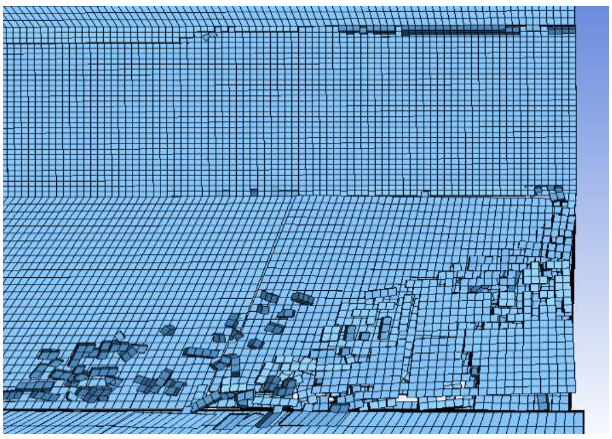

Fig. 2 Ice body fragmentation model

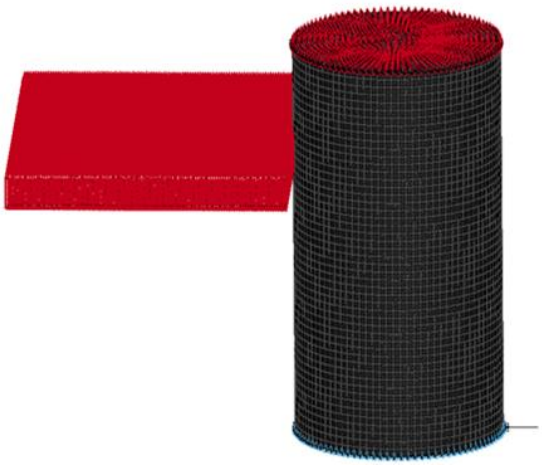

Fig. 3 Compressive strength and strain rate fitting curve

To improve computational efficiency, the grid size for the impact area is set to 0.20 m × 0.20 m × 0.20 m.

2.2 Pier Model

The pier uses the reinforced concrete model *MAT_PLASTIC_KINEMATIC proposed by Li et al. (2004) to simulate isotropy and strain hardening plasticity, which includes the rate effect to address the ice-induced vibration. The pier design features a double-column structure, common in the cold regions of our country, which experiences significant deformation due to ice pressure load. The single cylinder is taken as the study subject, and the response of the double-column pier to ice-induced vibration is expected to be more pronounced. According to investigations, during the dry season in spring, the water level of the Songhua River ranges from about 1.6 m to 7.2 m. In this simulation, the impact height is 7.2 m, the height of the pier is 10 m, and its radius is 3.6 m. To enhance computational efficiency, the model is simplified, and a grid size of 0.30 m × 0.30 m × 0.40 m is used for the pier. The grid standard adopted in this paper is the Warping Factor, with the average Warping Factor of the hexahedral grid of the pier being 0.16, which is below the warning level for solid elements. Therefore, the mesh size is considered feasible.

It should be noted that the simulation considers the highest water level during the low water period and simulates the most unfavorable conditions, but it somewhat neglects the influence of impact height on ice-induced vibrations. Furthermore, the structural dimensions of the pier, including its typical height and radius in the river, are chosen without exploring the effects of varying pier sizes on ice-induced vibrations. Therefore, this aspect should be addressed in future research. In this paper, through a fixed-height impact, the effect of water flow is verified in the simulation, and the related influence of the ice body is determined (Zhang, 2014).

Table 2 Calculation parameters of the concrete model

	Pier
Density/（kg/m^3）	2670
Young modulus/（GPa）	36
yield stress/（MPa）	35
Poisson ratio	0.2
Plastic damage strain/（MPa）	0.378×10^3

Due to the addition of a fluid-structured grid in the model, complexity significantly increases, making it easy for the negative contact volume to fail to converge. Therefore, the ice body is placed very close to the bridge pier to reduce calculation difficulty and improve efficiency. The contact algorithm in this paper adopts the penalty function method, and the contact types are *ERODING_SURFACE_TO_SURFACE and *ERODING_SINGLE_SURFACE.

2.3 Fluid-Solid Coupling Model

In the simulation of the pier-ice-water-air coupling collision, the coupling effects of the pier, ice, water, and air must be considered. This includes the interaction between the pier and ice, as well as between the fluid and the pier/ice body. Additionally, the effects of fluid resistance and the gravity field on the floating ice are taken into account. Specifically, the initial kinetic energy of the ice is transformed into an ice load, which leads to the vibration response of the bridge pier when it interacts with it. The core of the overall coupling setting focuses on four parts: boundary conditions, hydrostatic pressure, gravity field, and coupling settings. The boundary condition allows for the inflow and outflow of the fluid by utilizing local pressure gradient variations on the boundary. It also defines the boundary condition of the infinite field of the fluid and prevents the flow field's seepage problem. To simulate the hydrostatic floating of the ice body, hydrostatic pressure is applied to the flow field to maintain air pressure at 1 atmosphere, and water pressure varies with water depth. The gravity field is applied to the ice and piers through the gravity keyword. Then, when considering the reasonable floating state of the object, the ice body collides with the pier body. In this paper, the wind effect is not considered in the analysis, as it has little influence on the problems studied.

It should be emphasized that in the river, the flow velocity in the middle of the river is the fastest, and the flowing ice near the riverside will be subjected to the

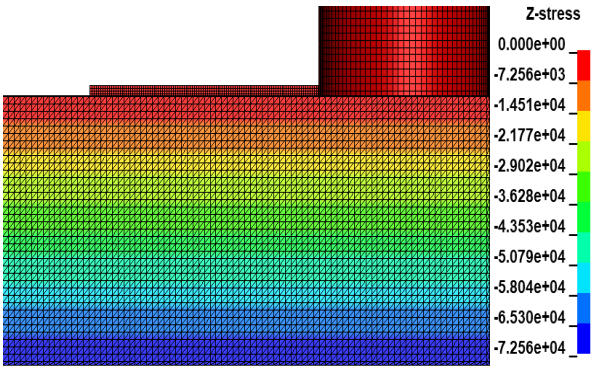

Fig. 4 Static hydraulic pressure initialization vector field (Pa)

resistance of the river bank and have less impact; thus, this paper focuses on the middle of the river. Therefore, for the boundary conditions of this research, taking the middle of the river as the research object, a non-reflection boundary is selected to simulate the actual situation in the center of the river.

In the process of fluid scour in this paper, the scour depth has a profound influence on the scouring of the fluid, but there is a fixed bearing connection at the bottom of the pier, and the direct scour effect of the fluid under the ice is minimal. Throughout the duration of the study, the cumulative scouring effect is very weak. At the same time, setting a shallow scouring depth can significantly reduce the calculation load. Therefore, this paper sets the entire research depth at 7.2 m, which is the same as the water depth. For depths close to 7.2 m, due to the connection mode at the bottom of the pier, the scouring effect is also very weak and can be ignored.

Regarding the fluid grid, computational efficiency is prioritized, and secondly, the mesh penetration effect, which is prone to occur in fluid analysis, needs to be addressed. To mitigate grid penetration, a grid size of 0.10 m × 0.10 m × 0.10 m is selected, balancing accuracy and computational efficiency. The wind effect is excluded from the analysis as it has minimal impact on the problems being studied.

LS-DYNA typically utilizes a constitutive model and an equation of state to describe fluid materials, such as air and water. In this paper, NULL material and *EOS_LINEAR_POLYNOMIAL are selected to simulate air and water, respectively. The dimensions of the water body are selected considering that the ice body has a minimal effect on the second half of the bridge pier after it breaks. According to simulation results and the actual situation, the ice body will develop cracks in the contact range following impact breakage. As the ice body penetrates deeper into the pier, these cracks continually expand, and the ice body itself also fractures with the expansion of these cracks. Consequently, its width is three times the diameter of the pier. The length is twice that of the ice body, and its height varies from about 1.6 m to 7.2 m, based on the investigation of the depth of the Songhua River during the low water period. The greater the impact height, the more pronounced the response to ice-induced vibrations of the pier, thus the height is set at 7.2 m. The height of the air domain extends from the water body to the top of the pier to simplify calculations and enhance computational efficiency.

Table 3 Fluid model calculation parameters

	Air	Water
Density/（kg/m^3）	1.25	1025
Failure stress/（Pa）	-1	-10
Stickiness/（N·s/m^2）	1.764 ×10^{-5}	8.684 ×10^{-4}
C_0	0	101325
C_1	0	2.25×10^9
C_2	0	0
C_3	0	0
C_4	0.4	0
C_5	0.4	0
C_6	0	0
E_0(Pa)	2.53×10^5	0
V_0	1	1

The materials for water and air are detailed in the table:

In *EOS_LINEAR_POLYNOMIAL, the internal energy in the linear polynomial equation of state is linear. The pressure is given by the following formula:

$$P = C_0 + C_1\mu + C_2\mu^2 + C_3\mu^3 + (C_4 + C_5\mu + C_6\mu^2)E$$

C_0 is the first coefficient of the polynomial equation, and C_1 is also the first coefficient of the polynomial equation (when used alone, this represents the elastic volume modulus; that is, it cannot be used for deformation beyond the elastic range), and so forth up to C_6, which is the sixth polynomial equation coefficient. V_0 represents the initial relative volume.

2.4 Comparison of Methods

In this paper, the fluid-solid coupling model can be divided into two categories in numerical simulation: boundary mapping and boundary non-mapping. The classical numerical method, the Arbitrary Lagrangian-Eulerian (ALE) algorithm, allows the grid on the boundary to move like a Lagrangian grid or remain fixed like an Euler grid, consistent with the solid. However, this method is typically suitable for simpler fluid-solid problems but exhibits many limitations in complex multi-body or three-dimensional problems. In LS-DYNA, the ALE algorithm primarily addresses the influence of fluid to solve fluid-solid coupling issues. In this algorithm, the relative velocity is introduced as the velocity of matter, and the conservation equations for mass, momentum, and energy are proposed. Then, the connection between the master contact surface and the slave contact surface is established using the penalty function method, enabling fluid-solid coupling. When penetration occurs, a series of springs are automatically set between the master contact surface and the slave contact surface to limit the penetration through spring force.

$$\frac{\partial \rho}{\partial t} = -\rho \frac{\partial v_i}{\partial x_i} - w_i \frac{\partial \rho}{\partial x_i}$$

$$\upsilon \frac{\partial v_i}{\partial t} = \sigma_{ij,j} + \rho b_i - \rho w_i \frac{\partial v_i}{\partial x_j}$$

$$\rho \frac{\partial E}{\partial t} = \sigma_{ij} v_{i,j} + \rho b_i v_i - \rho w_j \frac{\partial E}{\partial x_j}$$

Where ρ represents density, x_i denotes spatial coordinates, v_i stands for velocity components, and w_i b_i represents volume forces. σ_{ij} indicates the stress tensor, and E represents energy.

These three equations, detailing the conservation of mass, momentum, and energy in fluid dynamics, describe the changes in internal mass within the fluid, the movement and deformation under different conditions, and the energy transfer and distribution within the fluid, respectively. These equations form the foundational principles of the ALE method.

This paper adopts the more advanced S-ALE method in LS-DYNA/ANSYS software. The S-ALE method allows for free switching between Lagrangian and Eulerian coordinate systems during the simulation process. This method is based on the ALE approach but is more simplified and efficient than the traditional ALE method. The traditional ALE method requires users to define and generate detailed configurations during the preprocessing stage and then load them sequentially during computation. To enhance the efficiency and feasibility of large-scale fluid-solid coupling calculations, LS-DYNA introduces a new S-ALE algorithm, which improves upon the traditional ALE algorithm. The main difference is that the S-ALE algorithm simplifies the process of structural element modeling. Compared with the traditional ALE method, the S-ALE algorithm directly reads the geometric size and spacing information from the calculation file, thereby avoiding the need to load the nodes of all the elements used by the structured elements individually.

For this model, both the ALE and S-ALE methods are used to ensure that the corresponding end times and time steps are identical, and the final end time is calculated on the same computer.

In the actual experiment, the peak ice force on the pier facing the maximum ice sheet is 2432.82 kN, while in the simulation, the theoretical difference between the two methods is less than 10%. The difference with the ALE method is about 4.26% when the difference is 7.02%. It can be considered that the numerical simulation accurately reflects the impact effect of the actual situation.

Table 4 Comparison of two calculation methods

	ALE	S-ALE
Operate memory occupancy	74%	57%
Expected end time	33h28min	25h4min
Start solving the required memory (M)	31	19
Additional dynamic memory allocation (M)	790	555
Peak ice force calculation value(kN)	2603.61	2536.35

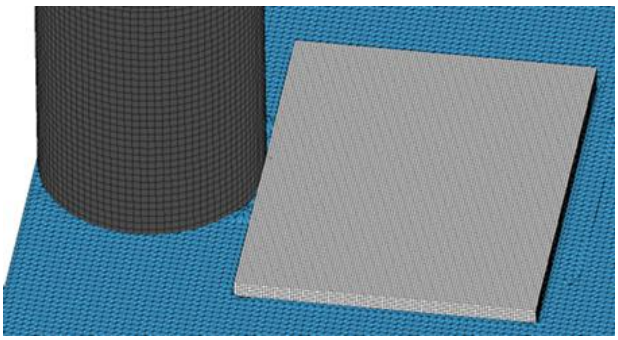

Fig. 5 Diagram of ice impact force on water surface

The S-ALE algorithm, in comparison to the traditional ALE method, offers a more reliable modeling approach, higher computational efficiency, a reduced memory footprint, and enhanced computing stability. These improvements make the S-ALE algorithm particularly promising for addressing large-scale flow-solid coupling problems. The method is well-suited for substantial deformations and severe displacements, especially under extreme conditions such as high-speed collisions, shocks, and explosions. It excels in accurately simulating the extensive coupling effects between fluids and solids. By editing the k-file, the S-ALE algorithm enables the structured grid to be saved as commands, which the solver can generate in real-time. This streamlines the calculation process and effectively distinguishes the impact and coupling problems. The ability to create structured grids dynamically during the simulation enhances flexibility and efficiency, contributing to a more effective and accurate representation of the complex interactions between fluids and solids in dynamic scenarios.

3. ANALYSIS OF THE OCCURRENCE MECHANISM OF ICE SHOCK VIBRATION AND THE VIBRATION RESPONSE UNDER FLOW-SOLID COUPLING

Based on the continuity of ice destruction processes, existing ice shock vibration dynamics models can be divided into two major categories. The first category was initially developed by Blenkarn (1970) and further expanded by Määttänen (1978). It is based on the negative damping mechanism. In this model, the damage from ice shock vibration is seen as a continuous crushing process. The moving ice force is calculated by the compression strength of ice, which is related to ice speed. Within a specific range, the ice speed exhibits a negative gradient, thereby providing negative damping to the structure and leading to structural dynamics instability and self-excited vibration. This model is simple and easy to use. The second model type assumes that ice destruction is intermittent, equivalent to the ice fragmentation frequency, which equals the ice speed divided by the characteristic length. Matlock first proposed an intermittent-damage dynamic model for ice, which reflects the general characteristics observed across all ice speed ranges in experiments, with small structural responses at low and high-speed ranges and significant responses in the medium speed range. However, it cannot

accurately predict ice shock vibration. This model is termed forced vibration. Sodhi (1994) modified Matlock et al. (1971) model to incorporate ice-structure interactions, including the loading phase of mutual contact, the crushing process of the ice plate, the structural ice removal process, and the separation process that may occur during ice-structure contact. Sodhi's model contains more process details and is more precise and reasonable. There is significant controversy over self-excited and forced vibration, and more thorough experimental and theoretical research is still needed.

In the spontaneous vibration model of continuous ice destruction, the interaction between ice and structure includes only the contact crushing process, and the ice force is considered the destructive ice force. This leads to the motion control equation for the entire process being simplified to a single degree of freedom spring oscillator and the ice body. The dynamic balance equation is obtained as follows:

$$m\ddot{x} + c\dot{x} + kx = F_f(t)$$

Where m represents the mass of the system, $\ddot{x}$ is the acceleration of the system (the second derivative of displacement with respect to time), c is the damping coefficient of the system, $\dot{x}$is the velocity of the system, k is the stiffness of the system, and $F_f(t)$ represents the ice-breaking force.

Furthermore, based on the Korzhavin formula, the magnitude of the ice-breaking force is formulated in the following function:

$$F_f = IqahD\sigma_f$$

In the mentioned equation, I q and a represent indentation, geometric, and contact coefficients, respectively. D is the diameter of the structure, h is the thickness of the ice, and σ_f represents the compressive strength of the ice. This correlation is illustrated in Figure 1. The compressive strength is determined by the strain rate, which satsfies:

$$\dot{\varepsilon} = \frac{v_t}{h}$$

Where v_t denotes the ductile-to-brittle transition rate, the relative velocity of the ice, and h is the thickness of the ice, significantly impacting dynamic ice forces. Thus, for small amplitude vibrations, the above equation can be formulated as follows:

$$m\ddot{x} + c\dot{x} + kx = F_f(v - \dot{x})$$

$$m\ddot{x} + c\dot{x} + kx = F_f(v) - \frac{\partial F_f(v)}{\partial v}\dot{x}$$

$$m\ddot{x} + (c + \frac{\partial F_f(v)}{\partial v})\dot{x} + kx = F_f(v)$$

If$\frac{\partial F_f(v)}{\partial v}$is set to c_i , then when the gradient in the ice force strain rate correlation curve is negative, the structure will undergo dynamic instability, leading to self-excited vibrations.

Self-excited vibration models typically treat the ice destruction process as continuous, but this assumption is only reasonable if the ice speed remains relatively constant. However, in the natural environment of a channel, ice speed tends to vary significantly, and the correlation curve of the ice destruction rate levels off at high loading rates. As shown in Figure 1, the negative damping effect is relatively weak under these conditions, leading to doubts about the validity of the self-excited vibration model. Structural dynamic parameters, such as the mechanics and destruction of ice, affect ice shock vibration differently by altering the ice speed range, position, and structural amplitude (Yue, et al., 2007). Additionally, there is a competitive relationship between the stochastic nature of ice destruction and the strain rate effect, which is crucial in generating ice shock vibrations. Ice shock vibration originates from the strain rate effect of ice destruction, and the mechanical mechanisms behind it include frequency modulation and an asymmetric positive feedback effect, which together amplify the kinetic energy transfer between the structure and the ice, thus leading to the occurrence of ice shock vibrations (Huang, 2021).

In this paper, the actual vibration situation can be reproduced in a controlled computing environment, and the analysis of the broken state of the ice body can determine which theory better describes the current vibration form in river conditions, thus providing a more comprehensive and quantitative evaluation of the applicability of the two theories on ice-induced vibrations.

3.1 The Form of Ice Damage

When the ice body impacts a bridge pier, there are generally four forms of damage: shock damage, extrusion damage, buckling damage, and bending failure (Hendrikse & Metrikine, 2016).

Impact ice force is one of the most common forms of river ice action on gravity piers. It demonstrates the impact of the ice flow on the bridge pier and stimulates the vibration response of the bridge structure. In shock damage, the ice force typically presents multiple separated peaks, and the instantaneous effect is powerful. Therefore, impact damage is significant in the effects of river flow ice on bridge piers. Another common form of ice force action is the crush-breaking ice force. When the ice flow exerts an extrusion effect on an upright hydraulic structure, a semi-elliptical area of damage forms at the front end of the ice plate. The damage gradually accumulates within this area until destruction eventually occurs. This type of crushing damage is also relatively common, especially in cases involving upright structures (Du, 2003). Impact and crush damage are two prevalent forms of ice force generated by river flow ice on piers or other hydraulic structures, which may trigger different types of structural responses and destruction mechanisms under various conditions.

For buckling damage and bending failure, when the ice flow is relatively thick upon colliding with the structure, it typically rises in the contact area. During this process, ice within a certain range experiences intense pressure, loses stability, and buckling damage may eventually occur. Here, the good mechanical properties of the ice flow lead to a bulge in the contact area. Conversely, the thick ice within the contact area may buckle

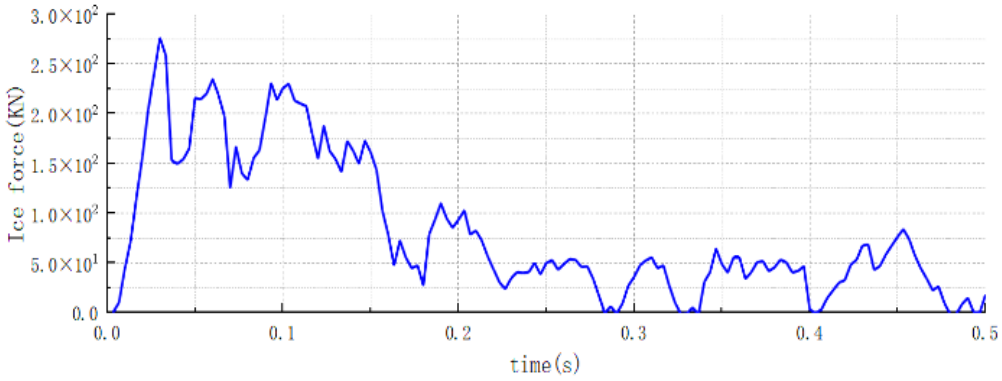

Fig. 6 Dynamic ice force time history curve (v=0.5 m/s, h=0.5 m)

and deform, eventually being destroyed in response to collision and compression. This damage often occurs together with extrusion damage in various combinations of damage forms. Buckling failure and bending failure are similar yet distinct (Yue, 2003). When the ice flow is thicker, it collides with the structure in the contact area, usually causing the ice within a specific range to suffer intense pressure, lose stability, and undergo buckling damage. Bending damage typically occurs before ice-breaking structures on inclined surfaces, such as the cone structure of an ocean platform and the tilted ice-breaking edges in front of inclined piers. In these cases, the destruction of ice flows exhibits brittle characteristics, prone to breaking and bending (Gürtner et al., 2009).

Because buckling failure is difficult to simulate, the bending failure form is not suitable for vertical cylindrical piers without ice-breaking prisms. Therefore, only the first two forms of destruction are simulated. Additionally, the disappearance of the failure unit may also cause a partial gap in the results.

3.2 Analysis of Ice Shock Vibration Response Under Fluid-Solid Coupling

Impact damage typically exhibits only 1 to 3 peak forces at the beginning of the impact. Hence, the simulation focuses on setting the initial speed in the impact direction without applying a driving force. In contrast, crush damage is a continuous process. To simulate the pushing of water and the rear ice flow during the extrusion process, uniform displacement can be applied to the back section of the ice flow, and the analysis time is set to 0.5 seconds. According to the simulation results, in the first stage, there is impact damage to the pier caused by the initial ice impact. Subsequently, the remaining ice is subjected to the water effect, continuing to squeeze the piers. During this process, central cracks form in the ice, and subsequent contact causes these cracks to propagate, forming a complete crack. In the second stage, the ice force peaks, and the dominant form of destruction emerges. Finally, in the third stage, the ice body is crushed and disintegrates, leaving the bridge pier, and ultimately, the ice force is completely unloaded. This paper specifically focuses on the ice shock vibration response of the pier body. The analysis involves examining the ice force-time curve of the pier body and the displacement-time curve of the upper part of the pier body. Considering real-world conditions, the ice flow rate is generally maintained within a range of 0.1 m/s to 2.5 m/s. The flow rate of the ice body is typically consistent with that of the water body by default. The average thickness of the ice body is set to 0.5 m.

As an example, when the speed is 0.5 m/s, the time course curve of the moving ice force is depicted in Fig. 6 below:

Analysis of causes

Based on the observation graph analysis, the process following the collision can be clearly defined. Initially, the ice body collides with the piers, resulting in a rapid peak in the ice force, usually accompanied by impact damage. Subsequently, cracks inside the ice body lead to a sharp decrease in the ice force. Then, with the current, the remaining ice bodies exert an extrusion effect on the piers. From the graphical observations, we observe that the dynamic ice load exhibits a typical "zigzag" feature over time, characterized by multiple smaller peaks between two significant ice force peaks. This pattern indicates that the destruction of ice bodies primarily takes the form of extrusion. This serrated response is evident throughout the ice force time curve, except during the initial phase, which does not cause crushing destruction of the ice body. When the cracks inside the ice body extend sufficiently, the ice force fails, and then the ice force acting on the bridge pier decreases sharply. It also happens that when the ice sheet hits the bridge pier, the ice speed slows down. Without failure, the ice force required for ice sheet destruction increases, causing it to be unbreakable and accumulate around the bridge pier, which then causes a subsequent ice force squeeze effect.

For the displacement curve of the pier, the ice-facing element at the top of the pier is selected by observing its displacement curve in the flow direction. When the flow direction is positive, the displacement time history curve of the pier top ice surface unit 7532 is shown in the following figure:

Analysis of causes

According to the image analysis, the interaction between the pier and the surrounding water body is clearly observable. When the ice force reaches its maximum, the pier does not quickly achieve maximum displacement but

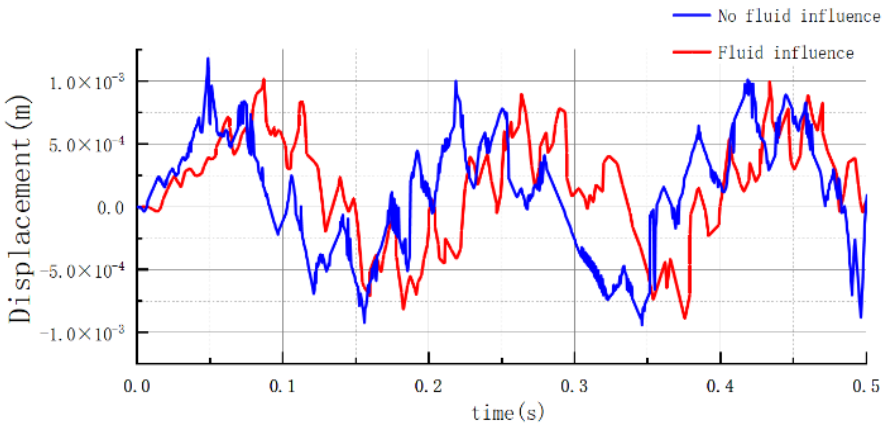

Fig. 7 Displacement time history curve (v=0.5 m/s, h=0.5 m)

experiences a subsequent squeezing effect. Especially when the flow direction is downward, the peak displacement of the ice-induced vibration response reaches 1.027×10^{-3} m, while it is only 0.8115×10^{-3} m in the reverse flow direction. Additionally, a single vibration period in the countercurrent direction shows a smaller amplitude and a shorter period, clearly reflected in the vibration between 0.202 s and 0.218 s in the figure. Regarding the basic amplitude, in the case of fluid influence, compared to the frequency without fluid influence, the average vibration period is significantly increased by 0.895 s and 31.3%. In terms of peak value, it increased by an average of 7.9%. These observations demonstrate that the action of water significantly affects the response of ice-induced vibration. Therefore, it is necessary to consider the fluid in the river, which will further explain the interaction mechanism between the river ice and the pier, contributing to a more comprehensive understanding of the relationship between the complex natural environment and the engineering structure.

The failure length of ice is about 0.1 to 0.5 times the ice thickness, with the average value being one-third of the ice thickness. There is no obvious relationship between failure length and the width-thickness ratio or the velocity-ice thickness ratio. The failure length of ice can be defined as:

$$\Delta l = ch$$

where h denotes the thickness of the ice body and c is the characteristic coefficient, generally ranging from 0.1 to 0.5, related to the characteristics of the structure and the scale effect. From the image, it is also observed that the ice force does not instantly drop to zero during the unloading phase, whereas there is a process. According to the failure length of ice, the characteristic frequency of the ice body can be obtained.

$$f_{\mathrm{i}} = \frac{\Delta l}{v_{\mathrm{i}}}$$

Before the actual structure, the failure length of ice under extrusion exhibits significant variability, so the ice force lacks clear periodicity. However, it usually conforms to a statistical law, meaning that the distribution within a certain frequency band exhibits specific regularity. The buckling and bending failures of ice show strong regularity, and the failure length from these types of failure is much longer than that from extrusion. Analysis of the formula reveals that when there is fluid influence, the velocity range of the ice body decreases, resulting in a characteristic frequency range that is slightly narrower than that of an ice body without fluid influence. This observation is consistent with the phenomenon observed in the figure.

In theoretical terms, the forced vibration theory can explain the observed phenomena, even under the influence of fluid. This theory elucidates the forced vibration characteristics of the bridge pier structure during intermittent ice breaking and the brittleness-ductility transition characteristics of the ice body at lower velocities. It is also consistent with brittle failure at higher speeds, resulting in continuous forced vibration caused by ice fragmentation. The results demonstrate that forced vibration theory effectively explains the vibration response of the river pier structure. These phenomena do not align completely with the theory of self-excited vibration, especially after the sudden velocity decrease in the first shock, where there is no clear frequency consistency. However, this may also be due to the short simulation time, the lack of obvious characteristics, and the fact that self-excited vibration requires a very narrow velocity range to trigger. Therefore, self-excited vibration still presents some limitations and warrants further exploration in a long-term theoretical dimension.

3.3 Analysis of Influencing Factors

In this paper, a speed range of 0-2 m/s with a fixed thickness is selected to simulate the peak of the moving ice force. The obtained data are shown in Figure 8 below:

Analysis of causes

According to the simulation results in this figure, as the speed of the ice body increases, its influence on the maximum ice force gradually diminishes. The data indicate that once the ice body speed reaches a certain level, the maximum ice force stabilizes at about 300 kN. This suggests that the main reason for the increase in peak impact force exerted by the ice body on the piers at lower velocities. However, once the speed reaches a specific critical value, the factors determining the peak size of the

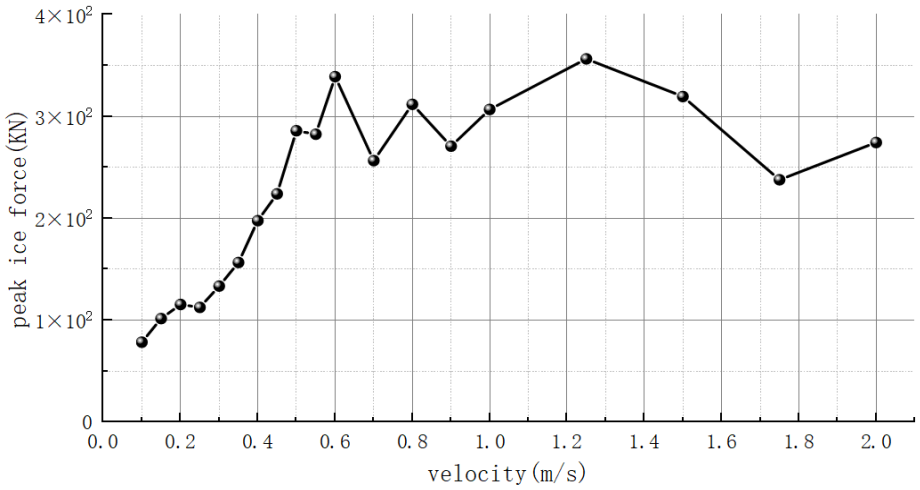

Fig. 8 Velocity-peak ice force plot (h=0.5 m)

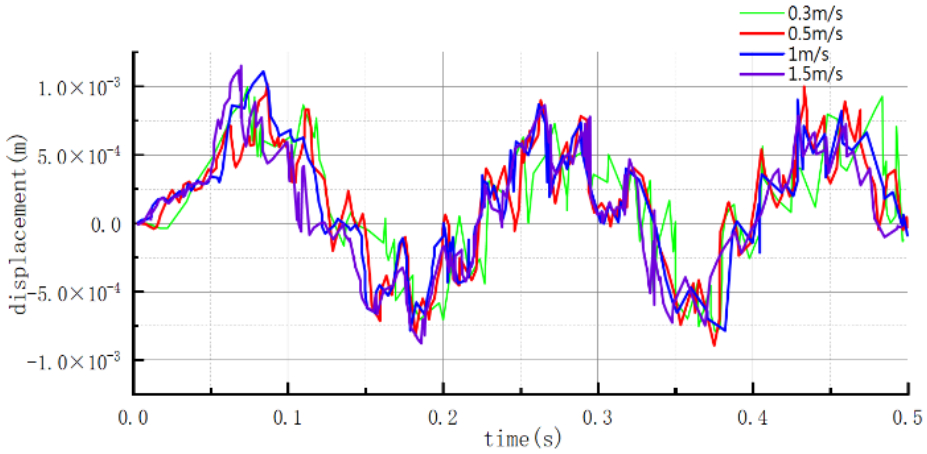

Fig. 9 Displacement time history curves for different velocity (h=0.5 m)

impact force are no longer predominantly influenced by speed but are governed by the strength properties of the ice body. Considering the toughness and brittle transition characteristics of the ice body, as the speed increases, the main form of ice destruction will gradually shift from toughness extrusion failure to brittle shock destruction. This damage process occurs primarily when the ice bodies contact the piers. It should be emphasized that in the numerical simulations, the ice body size selected in this paper is relatively small. In practical scenarios, when the scale of the ice body is large, its extruded ice force may be comparable to or even exceed the high-speed impact ice force. This result underscores the importance of considering both the size and velocity of the ice body in understanding the ice shock vibration response. The toughness and brittle transition properties of ice bodies, along with the behavioral differences in different sizes, significantly impact the vibration response. This facilitates a deeper understanding of the complexity of ice shock vibration phenomena and provides valuable insights for the design of related engineering structures. This observation also emphasizes the importance of comprehensively considering ice body properties and velocity factors in ice shock vibration research and engineering practice.

This paper selects 0.3 m/s, 0.5 m/s, 1 m/s, and 1.5 m/s four speeds to calculate the time course curve of the pier unit 7532 at the top of the ice surface, shown in Fig. 9 below.

Analysis of causes

Based on graphical observations, it can be determined that the displacement increase of the ice force within the velocity range of 1 m/s to 1.5 m/s is not significant. This observation aligns with the relationship between velocity and peak ice force. Conversely, at higher speeds, the considerable loading rate leads to the brittle failure of the ice material itself. This results in the continuous extrusion destruction of the ice row, and the zigzag extrusion ice force is less intermittent compared to the 0.3 m/s speed. The data reveals that the frequency of ice shock vibration response for faster ice bodies is higher, typically accounting for less than 15.7% of the cycle at the 0.3 m/s speed.

When the ice sheet causes extrusion before the occurrence of the vertical hydraulic structure, a semi-oval

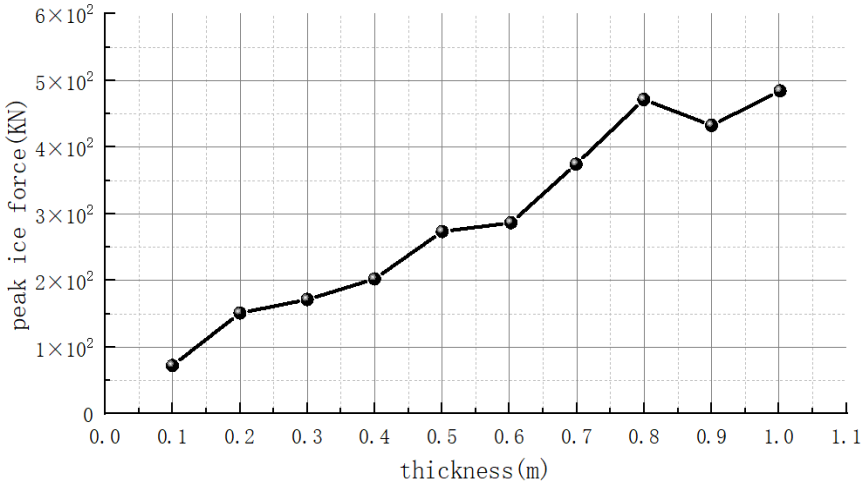

Fig. 10 Thickness-peak ice force plot (v=0.5 m/s)

damage area is formed at the front end of the ice plate, and the extrusion is the process from damage accumulation to damage. Because the mechanical properties such as toughness, brittleness, and ultimate strength of ice are strain rate-sensitive, the difference in ice velocity in front of a flexible structure will lead to a change in the action form. For the simulation process at four velocities, throughout the continuous process of collision and extrusion, it can be assumed that there is a three-dimensional strain field inside:

$$\varepsilon = \varepsilon(x, y, z)$$

Throughout this process, the strain field is a function of time and changes over time. The strain rate field in the stress region can be obtained by deriving the above equation:

$$\dot{\varepsilon} = \dot{\varepsilon}(x, y, z)$$

In the assumption of the strain field, x, y, z represent the coordinates in the water flow direction, transverse direction, and longitudinal direction respectively, with the extrusion direction x being the most significant. By simplifying the analysis, the stress zone can be regarded as a uniform one-dimensional elastic body, and the length of the force zone in the x-direction is defined as the length of the force zone. Then, the nominal strain rate of the force zone is:

$$\dot{\varepsilon} = \frac{v_r}{L_x}$$

Where v_r denotes the relative velocity between the ice sheet and the pier.

In front of the pier, the ice sheet's strain rate changes from low to high, and the extrusion is characterized by creep, quasi-static action, steady-state action, and random action. These correspond to the phenomena of creep, ductile failure, ductile-brittle transition failure, and continuous brittle failure of the ice body. This is consistent with the corresponding velocity in the image, and the failure mode also corresponds to the vibration pattern. However, after the collision, the velocity is lost, so the vibration patterns after the peak are also similar to each other.

The higher loading rates and speeds contribute to more frequent and intense ice shock vibration responses, indicating distinct dynamic behavior in the ice body under various impact conditions. Considering the width of the pier, another crucial factor influencing the ice body's impact is its thickness. In practical situations, the thickness of cold river ice bodies generally ranges from 0.1 m to 1 m. If the ice is too thin, its influence on the pier body will be exceedingly weak, making it irrelevant for study purposes. There is a relationship between peak ice force and thickness, as illustrated in Fig. 10.

Analysis of causes

The images illustrate a positive correlation between the thickness of the ice body and the peak ice force. This correlation can be attributed to two primary factors. First, the mass and momentum of the ice body increase with its thickness. When such an ice body collides with a structure, it transmits more kinetic energy, resulting in a higher peak ice force. Secondly, a thicker ice body possesses greater overall strength, making it more resilient to external impacts during collisions. Consequently, thicker ice bodies are less likely to break at the contact point, which contributes to a greater peak ice force.

In summary, the ice body's thickness significantly influences the peak ice force by affecting both the transfer of kinetic energy and the ice's structural integrity, enhancing its resistance to damage. Thus, there exists a proportional relationship between the thickness of an ice body and its peak ice force.

The results for ice thicknesses of 0.3 m, 0.5 m, and 1 m are depicted in Fig. 11:

Analysis of causes

The image illustrates that the impact force from an ice sheet with a thickness of 0.3 m is limited, and the ice breaks quickly, resulting in a weak vibration effect on the pier. However, when the thickness increases to 1 meter, the ice sheet's strength also increases, leading to a stronger impact force on the pier. Despite this increased strength,

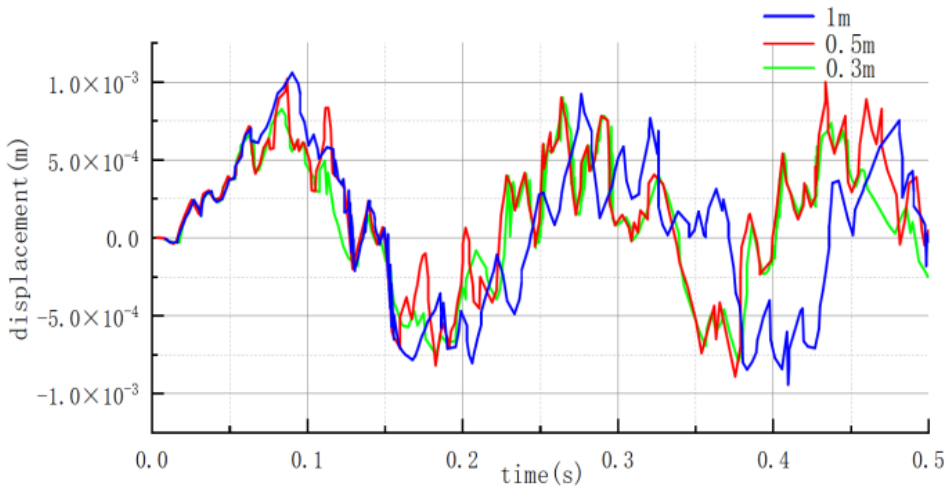

Fig. 11 Displacement time history curves for different thicknesses (v=0.5 m)

the degree of fragmentation is smaller, causing the ice-induced vibration effect on the pier to exhibit a peak value, albeit at a lower initial frequency. Due to the heightened strength of the ice body at a thickness of 1 meter, the cracks formed after the initial impact have a lesser effect on the overall integrity of the ice body. This increased strength also raises the difficulty of extrusion and crushing, leading to a prolonged vibration effect period. Conversely, the ice body with a thickness of 0.3 m breaks quickly, with the extrusion crushing force becoming predominant. The analysis of the mechanism reveals that the increased strength of the ice body impacts the loading rate and greatly enhances the compressive strength. Therefore, under a specific ice speed, the vibration frequency at a thickness of 1 meter is significantly lower than at 0.5 m, though the ice extrusion force becomes dominant later. Data analysis indicates that the vibration period for a thickness of 1 meter is 17% longer than that for 0.5 m, while the periods for 0.5 m and 0.3 m are more comparable.

It is hypothesized that the thickness of the ice body determines its strength, which in turn affects the form of failure and results in changes in ice-induced vibration. The figure shows that the sawtooth pattern is noticeably less pronounced in thicker ice, making it more difficult for destruction from the extrusion ice force to occur. In summary, the thickness of the ice sheet determines its overall strength and the mass energy of the impact, both of which significantly influence the response strength of the ice-induced vibrations.

This relationship is also supported by the empirical formula for ice force found in the "Code for Design of Railway Bridges and Culverts," which is part of the Chinese Bridge Design Code.

$$F_i = mC_i btR_{ik}$$

Where F_i and R_{ik} are the standard values of ice pressure and compressive strength. m , C_i are shape coefficient, ice temperature coefficient. b, t are facing the ice width, ice thickness. When there is a lack of measured data, R_{ik} is advisable to take 750kN/m^2, which can be obtained at this time.

$$F_i = mC_i btR_{ik} = 0.9 \times 1.1 \times 0.3 \times 2.5 \times 750 = 556.875kN$$

In the figure above, the ice force for a thickness of 0.5 m is only 176.8 kN, which is 31.7% of the result calculated by the formula. Similarly, for a thickness of 1 meter, it is 29.4% of the calculated result. It can be inferred that the results are roughly proportional. This indicates that although the strength of the ice body is lower than 750 kN/m^2, the thickness of the ice body does indeed enhance its compressive strength.

On the other hand, thickness also influences the ice body's tendency to break. The uneven distribution of the ice sheet, both in thickness and along the pier width, contributes to the randomness of the ice force. Due to the non-simultaneous failure during extrusion, the ice force value is much lower than that in "full contact" scenarios. Additionally, irregular and continuous brittle failure occurs on the ice face of the structure, with the timing and scale of breaking exhibiting significant variability. This results in strong randomness in the loading and unloading of ice pressure.

However, this paper has not established a quantitative relationship between these two influencing factors on ice-induced vibration response, which warrants further investigation.

4. Conclusion

In this paper, employing the LS-DYNA's S-ALE method, we analyzed the ice-induced vibration response of a river under fluid-solid coupling and identified two main factors influencing the response through numerical simulation. The following conclusions were drawn:

1. A simplified numerical simulation method for analyzing ice-induced vibration in rivers is introduced, considering the coupling of fluid dynamics and impact models. By comparing the S-ALE method with the traditional ALE method, it is observed that the computation time of the new method is reduced by 25.1%, and the memory usage is decreased by 22.97%. These findings highlight the significant advantages and potential

applications of the S-ALE method in complex fluid-solid coupling scenarios.

2. The flow velocity of the river significantly affects the response of ice-induced vibration. The duration of the ice-induced vibration caused by fluid dynamics is increased by about 30%, and the peak value is reduced by about 8%. Therefore, it is crucial to consider the influence of fluid dynamics on ice-induced vibration in rivers.

3. Regarding the applicability of vibration theory, the forced vibration theory can explain the observed phenomena, even under fluid action. This theory elucidates the vibration characteristics of bridge pier structures affected by water flow during intermittent ice breaking. The results confirm the broad applicability of forced vibration theory under conditions of ice-induced vibration in rivers.

4. Concerning the factors affecting ice-induced vibration: ice speed and ice thickness are the main determinants. Ice speed influences the initial peak ice force of impact, while ice thickness determines the strength and failure characteristics of the ice. Although higher speed has a minimal impact on the vibration response, it increases the frequency of pier vibrations. There is a non-linear relationship between ice thickness and ice force; lower thicknesses show a similar effect, whereas greater thickness significantly amplifies the vibration effect.

ACKNOWLEDGMENTS

The responsibility for the information released within this section is entirely on the corresponding author.

CONFLICT OF INTEREST

All authors disclosed no relevant relationships. The author(s) declared no potential conflicts of interest with respect to the research, author- ship, and/or publication of this article.

AUTHORS' CONTRIBUTIONS

Zhang Zhonghao: Formal analysis, Funding acquisition, Resources, Software, Supervision; **Song Jiahao:** Conceptualization, Investigation, Project administration, Visualization, Writing-original draf; **Wang Kexin:** Data curation, Methodology, Validation, Writing-review & editing.

REFERENCES

Blenkarn, K. A. (1970). *Measurement and analysis of ice forces on cook inlet structures*. Offshore Technology Conference, Houston, 365-378. *https://doi.org/10.4043/1261-MS*

Cai Z. R., Feng, Y. H., Meng, X. Y. (1995). Ice Load of Flowing-Ice Impacting Jiamusi Highway Bridge in 1995. *World Earthquake Engineering, 1995*(04), 55-57. CNKI:SUN:SJDC.0.1995-04-009

Devinder, S. S. (2001). Crushing failure during ice–structure interaction. *Engineering Fracture Mechanics, 68*(17), https://doi.org/10.1016/S0013-7944(01)00038-8

Dong, J. W. (2012). *Physical simulation study on the action of sea ice on circular piles and sloped structures and their protection facilities* [Doctoral dissertation, Dalian University of Technology].

Dong, J. W., Li, Z. P., Lu, P., Jia, Q., Wang, G. Y., Li, G. W. (2011). Design ice load for piles subjected to ice impact. *Cold Regions Science and Technology, 7*(1). https://doi.org/10.1016/j.coldregions.2011.11.002

Du, X. (2003). *Research on dynamic ice force of flexible vertical structures* [Master's thesis, Dalian University of Technology]. Dalian. https://doi.org/10.7666/d.y666827

Gürtner, A., Bjerkås, M., Kühnlein, W., Jochmann, P., & Konuk, I. (2009). Numerical simulation of ice action to a lighthouse. *ASME 2009 28th International Conference on Ocean, Offshore and Arctic Engineering*, American Society of Mechanical Engineers, 175-183. https://doi.org/10.1115/OMAE2009-80164

Hendrikse, H., & Metrikine, A. (2016). Ice-induced vibrations and ice buckling. *Cold Regions Science and Technology, 131*, 129-141. https://doi.org/10.1016/j.coldregions.2016.09.009

Huang, G. (2021). Lock-In resonance analysis in ice-induced vibration. *Chinese Journal of Theoretical and Applied Mechanics, 53*(03), 693–702. https://doi.org/10.6052/0459-1879-21-087

Jordaan, I. J., & Timco, G. W. (1988). Dynamics of the Ice-Crushing Process. *Journal of Glaciology, 34*(118), pp. https://doi.org/10.3189/S0022143000007085

Karna, T., & Turunen, R. (1989). Dynamic response of narrow structures to ice crushing. *Cold Regions Science and Technology, 17*(2), 173-187. https://doi.org/10.1016/S0165-232X(89)80007-2

Kashfi, B. H., Taylor, R. S., Bruneau, S., & Jordaan, I. J. (2015). *Experimental study of dynamics during crushing of freshwater truncated conical ice specimens.* Proceedings of the ASME 34th International Conference on Ocean, Offshore and Arctic Engineering, 2015, Vol 8. *https://doi.org/10.1115/OMAE2015-41904*

Kehua, Y., Chun, L., Yang, Y., Wanfu Z., & Zifei X. (2019). Research on the influence of ice-induced vibration on offshore wind turbines. *Journal of Renewable and Sustainable Energy, 11*(3), https://doi.org/10.1063/1.5079302

Kennedy, K. P., Jordaan, I. J., Maes, M. A., & Prodanovic, A. (1994). Dynamic activity in medium-scale ice indentation tests. *Cold Regions Science and Technology, 22*(3), https://doi.org/10.1016/0165-232X(94)90004-3

Li, Z., Jin, F., & Cai, Z. (2004). Free vibration

characteristics and dynamic response of concrete slabs. *Proceedings of the 9th Academic Annual Meeting of China Civil Engineering Society Protective Engineering Branch*, Changchun, 415-420.

Määttänen, M. (1978). *On conditions for rising self-excited ice-induced autonomous oscillations in slender marine pile structures.* https://www.traficom.fi/sites/default/files/10708-No_25_On_conditions_for_the_rise_of_self-excited_ice-ind.p

Matlock, H., Dawkins, W. P., & Panak, J. J. (1971). Analytical model for ice-structure interaction. *Engineering Mechanics, ASCE*, *97*(4), 1083–1092. https://doi.org/10.1061/JMCEA3.0001434

Ou, J., Wang, G., & Duan, Z. (2002). Ice force model of offshore platform structures. *Ocean Engineering*, *2002*(01), 7-14. https://doi.org/10.16483/j.issn.1005-9865.2002.01.002

Oxford (2018). *Research on the interaction between river ice and bridge piers in cold regions* [Master's thesis, Harbin Institute of Technology]. https://doi.org/CNKI:CDMD:2.1018.894544

Qu, Y. (2006). *Stochastic ice load analysis on offshore structures based on in-situ experiments* [Doctoral dissertation, Dalian University of Technology]. https://doi.org/10.7666/d.y865980

Rice, J. R., & Thomson, R. (1974). Ductile versus brittle behavior of crystals. *Philosophical Magazine*, *29*(1), 73–97. https://doi.org/10.1080/14786437408213555

Sodhi, D. S. (1994). *A theoretical model for ice-structure interaction.* Proceedings of the OMAE-94 Conference, ASME, New York, Volume IV, Pages 29–34. *A Theoretical Model for Ice-Structure Interaction (iahr.org)*

Sodhi, D. S., & Morris, C. E. (1986). The characteristic frequency of force variations in continuous crushing of sheet ice against rigid cylindrical structures. *Cold Regions Science and Technology*, *12*(1), https://doi.org/10.1016/0165-232X(86)90015-7

Wang, J. (2017). *Research on the method of obtaining design parameters when sea ice acts on structures* [Master's thesis, Dalian University of Technology]. https://doi.org/CNKI:CDMD:2.1017.822574

Xu, J., & Erkan, O. (2018). The physical mechanism of ice/structure interaction. *Journal of Glaciology*, *64*(244), https://doi.org/10.1017/jog.2018.5

Yin, H. B. (2019). Impact analysis of floating ice bridges and research on anti-collision devices [D]. Harbin Institute of Technology, 2019. https://doi.org/10.27061/d.cnki.ghgdu.2019.000923.

Yu, T., Lei, J., Shan, S., & Yuan, Z. G. (2011). Research on the calculation model of river ice floes impact on bridge piers in spring. *Vibration and Shock*, *30*(06), 192-195. https://doi.org/10.3969/j.issn.1000-3835.2011.06.039

Yue, Q. J., Ren, X. H., & Chen, J. B. (2005). Experimental and mechanism study on brittle-ductile transition of sea ice. *Journal of Applied Basic Science and Engineering*, *2005*(01), 35–42. https://doi.org/10.3969/j.issn.1005-0930.2005.01.005

Yue, Q., & Bi, X. (2000). Ice-induced jacket structure vibrations in bohai sea. *Journal of Cold Regions Engineering*, *14*(2), 81–92. https://doi.org/10.1061/(ASCE)0887-381X(2000)14:2(81)

Yue, Q., & Bi, X., & Yu, X. (1999). *Full-scale tests and analysis of dynamic interaction between ice sheet and conical structures.* https://www.iahr.org/library/infor?pid=27555

Yue, Q., & Bi, X., & Yu, X. (2003). Ice-induced vibration and ice force function of conical structures. *Journal of Civil Engineering*, *2003*(02), 16-19. CNKI:SUN:TMGC.0.2003-02-003

Yue, Q., Guo, F. W., & Tuomo K. (2008). Dynamic ice forces of slender vertical structures due to ice crushing. *Cold Regions Science and Technology*, *56*(2), https://doi.org/10.1016/j.coldregions.2008.11.008

Yue, Q., Guo, F., Bi, X. (2007). Measurement and mechanism explanation of ice-induced self-excited vibration. *Journal of Dalian University of Technology*, *2007*(01), 1–5. https://doi.org/10.3321/j.issn:1000-8608.2007.01.001

Zhang, S. (2014). *Interaction between Flowing Ice and Bridge Piers* [Doctoral dissertation, Northeast Forestry University]. Harbin.

Zhu, B., Sun, C., & Jahangiri, V. (2021). Characterizing and mitigating ice-induced vibration of monopile offshore wind turbines. *Ocean Engineering*, *219*, https://doi.org/10.1016/j.oceaneng.2020.108406